SWST 63rd
July 12-15, 2020

Preparation of cellulose acetate-polyacrylonitrile composite nanofibers by multi-syringe electrospinning method: morphology, wettability, and mechanical properties

Dong Wang, Wanli Cheng, Qingxiang Wang, Guangping Han*

College of Material Science and Engineering, Northeast Forestry University, Harbin, Heilongjiang, China, 150040

Introduction

Electrospun cellulose acetate-polyacrylonitrile (CA-PAN) nanofibrous membranes with controllable spatial structure were fabricated by a multi-fluid mixing electrospinning process. SEM showed that morphologies of membranes transformed from smooth to rough surface upon changing the weight ratios of CA to PAN, whereas their average diameters increased from 303 to 502 nm. The static contact angle value of membranes increased from 86 to 131° with increase in CA content. The hydrophilic-hydrophobic properties were affected by the "mixture rule" of surface microstructure and spatial structure. The PAN nanofibers had higher elongation at break (εb), however their yield strengths were lower, while CA fibers exhibited poor mechanical properties. After introduction of CA fibers into CA-PAN membranes, the mechanical properties were improved significantly. The 33%CA(67PAN) nanofibers showed highest tensile strengths (max, 5.0 MPa) and εb (29.2 %) values. Moreover, the composition, roughness and thermal stabilities of nanofibers were also analyzed. The structure-property relationship was clarified.

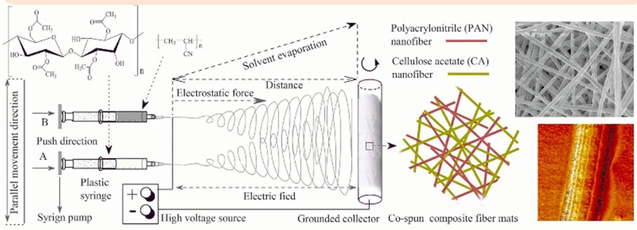

Methods

A 10 wt% solution of CA in DMAc/acetone (1/1) mixture was prepared, and stirred at 25° C until it became homogeneous. A 14 wt% solution of PAN in DMF was also prepared by stirring for 24 h at 50 ° C. The CA-PAN nanofibers membranes were prepared using a SS-2535H electrospinning device (Yong Kang Le Ye Co., Beijing, China). The solution was loaded into 10 mL syringes, each provided with a 17G needle (i.d.: 1.12 mm).

The CA and PAN spinning solutions, which were loaded into different syringes, were placed in their respective A and B positions of syringe pump device as shown in Fig. 1. The ratios of CA to PAN were adjusted to 33/67, 50/50, 67/33, and 75/25 (w/w) by controlling the number of syringes in A or B positions of syringe pump device. The spinning rates for A and B were 0.35 mm/min and 0.25 mm/min, respectively. Constant high positive and negative voltages generated by a power supply were applied between the syringe needles (+16.70 kV) and the roller collector (-2.70 kV) covered with aluminum foil. The speed of roller collector was set to 100 rpm and its distance from the needle tip was 22 cm. The humidity and temperature were kept at 22% and 25 ° C in all experiments.

Results

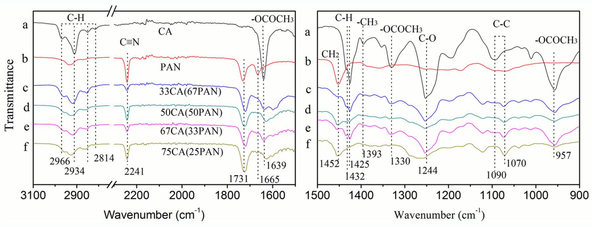

Fig. 1. FTIR curves of CA-PAN membranes with different weight ratios of CA fibers to PAN fibers

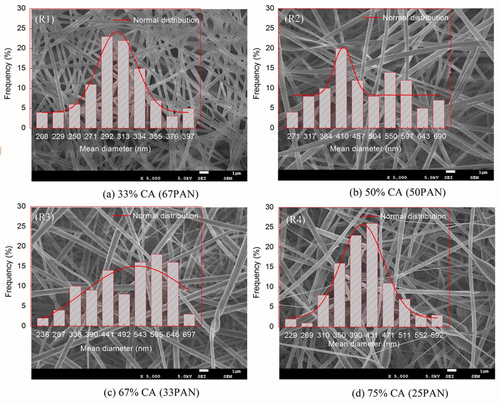

(a) 33% CA (67PAN) (b) 50% CA (50PAN) (c) 67% CA (33PAN) (d) 75% CA (25PAN)

Fig. 2. SEM of electrospun CA-PAN composite nanofibers with different weight ratios of CA to PAN. The inset images represented the average diameters and size distributions of the electrospun CA-PAN nanofibers

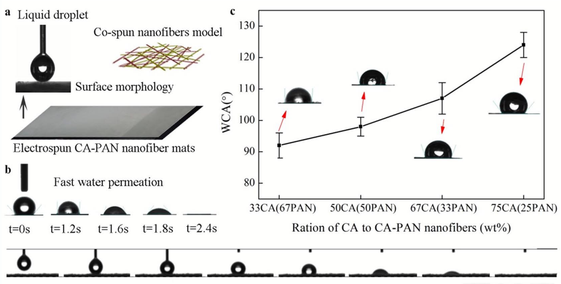

Fig. 3. Determination of wettability of CA-PAN nanofiber mats. (a) Photographs of co-spun CA-PAN nanofibers and its surface morphology. (b) Dynamic photograph of water permeation on the surface of the 50%CA(50PAN) fibers. (c) Variations in WCA of CA-PAN fibers with increasing CA concentration.

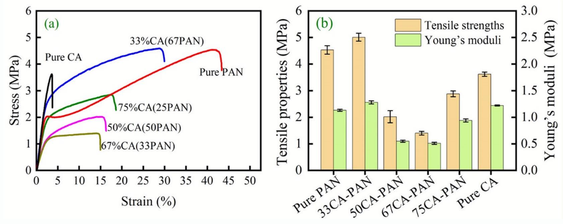

Fig. 4. Stress-strain curves (a) and tensile properties (b) of electrospun CA-PAN composite nanofibers with different weight ratios of CA to PAN

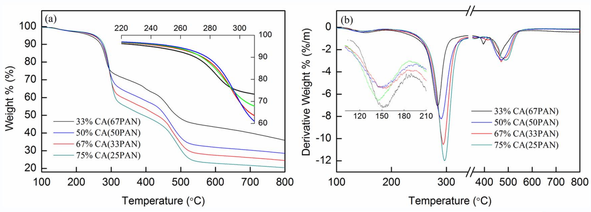

Fig. 5. The (a) TG and (b) DTG curves of electrospun CA-PAN composite nanofibers

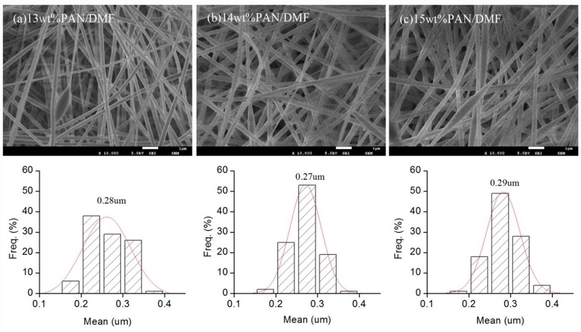

Fig. S2. SEM images of electrospun nanofibers of (a) 13wt% PAN, (b) 14 wt% PAN, and (c) 15wt% PAN. The bottom images represented the measured average fiber diameters and size distribution of the electrospun PAN fibers.

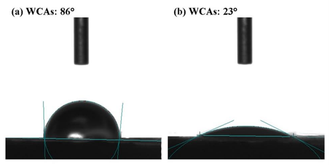

Figure S3. Characterization of wettability of 14wt% PAN nanofibers: Photographs of WCAs on the surface of nanofibers at (a) 0s and (b) 30s.

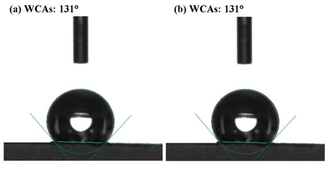

Figure S4. Characterization of wettability of 10 wt% CA nanofibers: Photographs of WCAs on the surface of nanofibers at (a) 0s and (b) 30s.

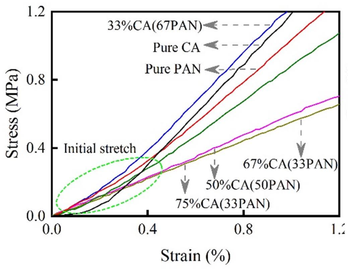

Figure S5. Initial stress-strain curves of electrospun CA-PAN composite nanofibers with different weight ratios of CA to PAN

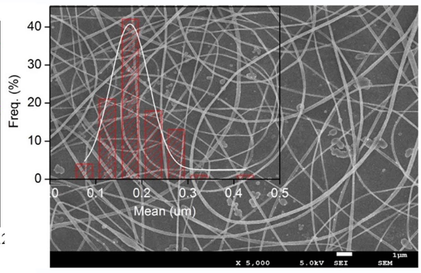

Fig. S1. SEM images of electrospun nanofibers of 10 wt% CA and its fiber diameter and size distribution.

Conclusions

A series of CA-PAN composite nanofibers with controllable spatial structure were was successfully fabricated using multi-syringe electrospinning process. FTIR analysis indicated that the CA and PAN nanofibers were physically interconnected and did not react chemically during electrospinning. Moreover, the spatial structure between nanofibrous membranes changed with increase in the proportion of CA nanofibers in CA-PAN composites nanofibers. The average diameter of nanofibers increased gradually, showing numerous nano-scaled roughness and uneven diameter distribution. Interestingly, the WCA of composite nanofibers increased from 92 to 128° with increase in CA fiber content from 33 to 75%. This suggested increase in hydrophobicity and lowering of water permeability with increase in CA content. This could be ascribed to the "Mixture Ruleof low adhesion of nanofibers with water and spatial structure of CA and PAN nanofibers. In addition, the mechanical properties of nanofibers were also affected by the synergy between nanofiber morphology and spatial structure.

After introduction of CA fibers into the composite nanofibers, the mechanical properties significantly improved. The 33%CA(67PAN) composite nanofibers showed the best mechanical properties (E, 1.28 MPa, σmax 5.0 MPa, and εb 29.2%). The 75%CA(25PAN) composite nanofibers could be used in the field of membrane separation, considering their hydrophobicity and mechanical properties. The thermal stabilities of electrospun CA-PAN membranes were only related to the inherent properties of fibers and independent from the spatial structure. This design demonstrated the potential applications of the fabricated nanofiber composite materials in membrane separation applications.

Acknowledgements

This work was financially supported by the National Natural Science Foundation of China (Grant No. 31470580) and the Fundamental Research Funds for the Central Universities (Grant No. 2572019AB02).